Integrated Concentrating Solar/Photovoltaic Hybrid Concepts—Technological Discussion, Energy Yield, and Cost Considerations

Moritz Ruhwedel, Kai Gehrke, Eckhard Lüpfert, Florian Sutter, Peter Heller, and Robert Pitz-Paal*

Concentrating solar thermal (CST) technologies are a sustainable way to produce high-temperature heat. Four concepts of integrating photovoltaics (PV) into CST plants, namely Rear-PV, PV-Mirror, bifacial PV-Mirror and Spillage-concentrating PV (CPV), are compared and the technological and economic outcome is discussed. The concepts are presented for the use with solar tower systems, but can also be applied to other configurations. In this work, parameters for each concept to quantify annual energy production and investment costs are derived. It is determined that implementing Rear-PV, PV-Mirror, bifacial PV-Mirror, and Spillage-CPV in a concentrating solar power tower plant leads to an additional energy yield as high as 23%, 29%, 40%, and 36%, respectively, on the same mirror aperture size. For the concepts of the Rear-PV, PV-Mirror, and bifacial PV-Mirror, maximum allowable cost per aperture area can be 3.0, 4.8, and 5.7 times the cost of conventional mirrors, to reach a break-even of the specific investment cost per annually produced energy. Such values are considered to be achievable for PV-Mirror and bifacial PV-Mirror, but not for Rear-PV. For Spillage-CPV, a break-even of investment cost can be achieved if installed in areas with spillage radiation flux exceeding ≈350 kWm^{-2} at peak.

1. Introduction

Concentrating solar thermal (CST) technologies supply sustainable heat to a variety of applications, like air-conditioning in buildings, domestic heat, industrial process heat, and chemistry. In the important CST subfield of concentrating solar power (CSP), the heat drives a thermodynamic power cycle. CSP competes with photovoltaics (PV) in commercial solar electricity production. The levelized cost of electricity (LCOE) of large-scale PV power plants is currently estimated to be ≈50% lower than the LCOE of CSP.[1] But as an important advantage, CSP allows to easily integrate thermal storage, and for storage periods longer than 4–10 h CSP is expected to remain the cheaper option compared to PV in combination with battery or thermal storage.[2] Since energy storage is critical to achieve a high share of renewable electricity, CSP will be a relevant technology. Increased amount of installations will lead to LCOE decrease also for CSP.

One path to systematically increase the cost-competitiveness of CST technology is the exploitation of unused potentials by combining it with PV. In this work, four combined CST/PV concepts are compared: concept #1, the Rear-PV,[3–5] concept #2, the PV-Mirror,[6–11] concept #3, the bifacial PV-Mirror,[9] and concept #4, the Spillage-concentrating PV (CPV).[12,13] The goal of this work is to derive parameters for these four concepts for their quantitative comparison in terms of energy production and investment costs. In the following, first these concepts are described. Then, their technological aspects are discussed. Finally, their energy yield and cost are estimated and compared.

2. Introduction of the CST/PV Hybrid Concepts

2.1. Losses in CST Applications and PV

The core idea of the hybrid concepts is to reduce losses in CST applications and PV by combining them. Therefore, the relevant losses of these technologies are explained in the following. In **Figure 1**, the relevant losses in CST applications are summarized.

M. Ruhwedel, E. Lüpfert, F. Sutter, P. Heller, R. Pitz-Paal
Deutsches Zentrum für Luft- und Raumfahrt (German Aerospace Center DLR)
Institute of Solar Research
Linder Höhe, Köln 51147, Germany
E-mail: Moritz.Ruhwedel@dlr.de

M. Ruhwedel, R. Pitz-Paal
Chair of Solar Technology
RWTH Aachen University
Linder Höhe, Köln 51147, Germany

K. Gehrke
Deutsches Zentrum für Luft- und Raumfahrt (German Aerospace Center DLR)
Institute of Networked Energy Systems
Carl-von-Ossietzky-Str. 15, Oldenburg 26129, Germany

The ORCID identification number(s) for the author(s) of this article can be found under https://doi.org/10.1002/ente.202301181.

DOI: 10.1002/ente.202301181

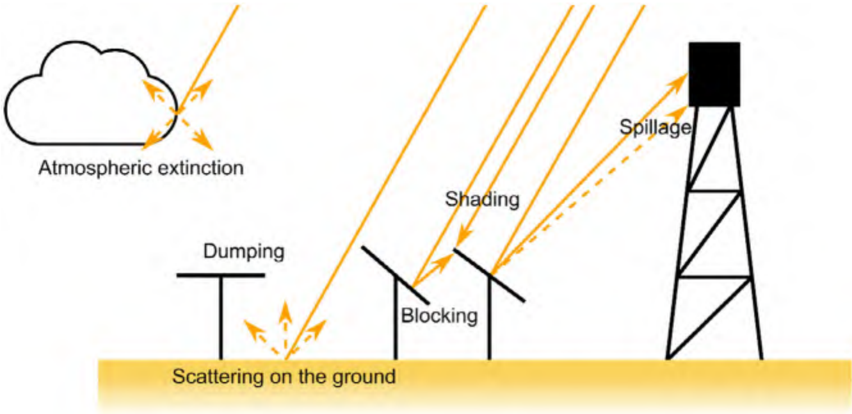

Figure 1. Losses of incident power in a central receiver system.

Atmospheric extinction refers to the attenuation of the extraterrestrial solar radiation due to scattering and absorption as the sunlight passes through the atmosphere. Part of the scattered light is available on the ground as diffuse radiation from the sky. Concentrating solar systems, however, cannot concentrate diffuse radiation. In addition, in central receiver systems (CRSs) atmospheric extinction also reduces the energy reflected from the heliostat field on its path to the central receiver.[14] In particular, atmospheric extinction contributes to the fact that the optical efficiency of heliostats becomes lower the further away from the receiver they are located. Due to the short focal distance, in parabolic trough collectors (PTCs) or linear Fresnel collectors (LFCs), the influence of atmospheric extinction is negligible.

Of the total solar radiation falling on the field of the CST system, only the fraction hitting the mirrors can be used. The rest hits the ground and is absorbed or scattered. The scattered light can be available again as diffuse radiation, also at the backside of the mirrors. The amount of power available this way is mainly determined by the ground coverage ratio (GCR) and the ground albedo. The GCR is defined as ratio of the (mirror) aperture area to the field area. The ground albedo quantifies how much light is reflected at the ground.

The concentrated solar radiation not hitting the receiver in CST applications is called spillage. This is due to shape or tracking deviations of the heliostat mirrors, as well as the beam width of the sunlight, both affecting the system performance. The further away from the receiver the heliostats are positioned, the wider the focal spot gets on the receiver, and the greater this loss. Receiver aperture dimensions are important, as well as heliostat quality and heliostat packing in the field. Field layout and receiver dimensioning affect how much energy falls into the receiver aperture.[15] Spillage radiation flux of up to few hundred kWm^{-2} are reached in CRSs. While fractions in the single-digit percentage range are common for cylindrical receivers, fractions of several tens of percent can be reached for high-temperature receivers.

Shading refers to the shadow cast by one mirror on the surface of another.

Blocking refers to the situation when the radiation reflected from one mirror toward the receiver is blocked by the back of another mirror. This can occur in both CRSs and LFCs, but not in PTCs where a receiver is illuminated by only one continuous mirror surface. Both shading and blocking occur more in solar fields when dense packing (high GCR) is an objective.

Dumping is the term for situations when more solar energy is available than receiver or downstream systems can take, and part of the mirror field is defocused. The amount depends on the degree of solar field oversizing in the design of the system to achieve high solar shares.

Solar energy remains also lost during times of maintenance and other system outages, as well as during times with too low direct normal irradiance (DNI), e.g., covering system loss or starting turbine operation, in particular in the morning and evening and during overcast skies.

While the CST efficiency in principle does not depend on the wavelength of the utilized radiation, for PV, a wavelength dependence of the efficiency depends on the bandgap of the cell material: photon energies below the bandgap cannot be utilized. Of photon energies above the bandgap, only the bandgap energy can be utilized, the remaining energy is dissipated in the cell as heat.

As the operating temperature of PV cells increases, their efficiency decreases. This effect is approximately linear and is described by the temperature coefficient. For silicon cells, it is below $-0.4\%\ K^{-1}$ depending on the cell technology.

In arrays of PV cells, partial shading reduces the efficiency of the system as it leads to mismatching of the maximum power points of the single cells.

2.2. The Concepts

In addition to the typical approach of combining CSP and PV in adjacent but separate fields with common infrastructure, PV can be integrated into a CST system either in the non-concentrated part, i.e., the collecting structure, or in the concentrated part at the receiver (CPV). In the past, when PV used to be very expensive, primarily the latter option was investigated as it requires only a small module surface area.[16] Mainly the parallel use of thermal and PV receivers by spectral beam splitting was investigated. These concepts have not made it to wider commercial

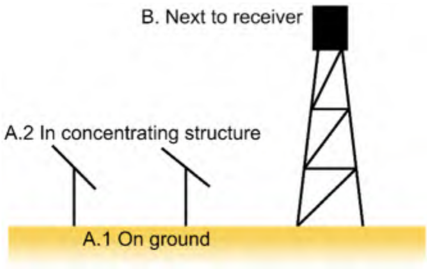

Figure 2. Mounting locations for PV cells in CST systems: on the ground A.1), in the concentrating structure A.2) and next to the receiver B).

application. As nowadays PV modules are much cheaper, the application of PV in the non-concentrated part is increasingly investigated. It can be subdivided into the application on the ground between the mirrors and the application on the mirrors. The possible mounting locations are shown in **Figure 2**.

By mounting the PV on the ground, the radiation that does not hit the mirrors could be utilized. This option is not considered here as the space around the mirrors is needed for cleaning and maintenance of the mirror system. Furthermore, land costs make up only a small part of the cost of large CST applications[17]—PV could rather be placed on additional sites instead.

If the PV is integrated in the concentrating structure and the mirrors are replaced, the reflectance of the concentrating aperture area might differ from the reflectance of conventional solar mirrors. In this case, the ideal power plant configuration also changes, i.e., in the CRS example the receiver size, the associated components and the layout of the heliostat field. This effect is nonlinear: for example, in a CSP plant, increasing the reflectance of the mirrors allows for higher mass flow rates of the heat transfer medium while keeping the outlet temperature constant. Thus, the share of heat losses decreases.

In this work, four hybrid CST/PV concepts are compared, three of which replace the conventional mirrors. They are shown in **Figure 3** and explained in the following.

2.2.1. Rear-PV

Mirrors with PV on their back are used. During normal operation, the diffuse radiation and the blocked radiation hitting the backside can be utilized. Whenever a mirror is not needed to concentrate radiation, i.e., during dumping, low DNI, or maintenance, it can be turned backside up, so that the PV faces the sun, as far as the tracking system allows. For most commercial heliostat designs, this flipping is not possible.

2.2.2. PV-Mirror

PV cells with a spectrally selective mirror on top replace the conventional mirrors. The spectrally selective mirror transmits wavelengths that the PV cells can efficiently utilize, while the rest of the spectrum is reflected to the CST receiver. Diffuse radiation is

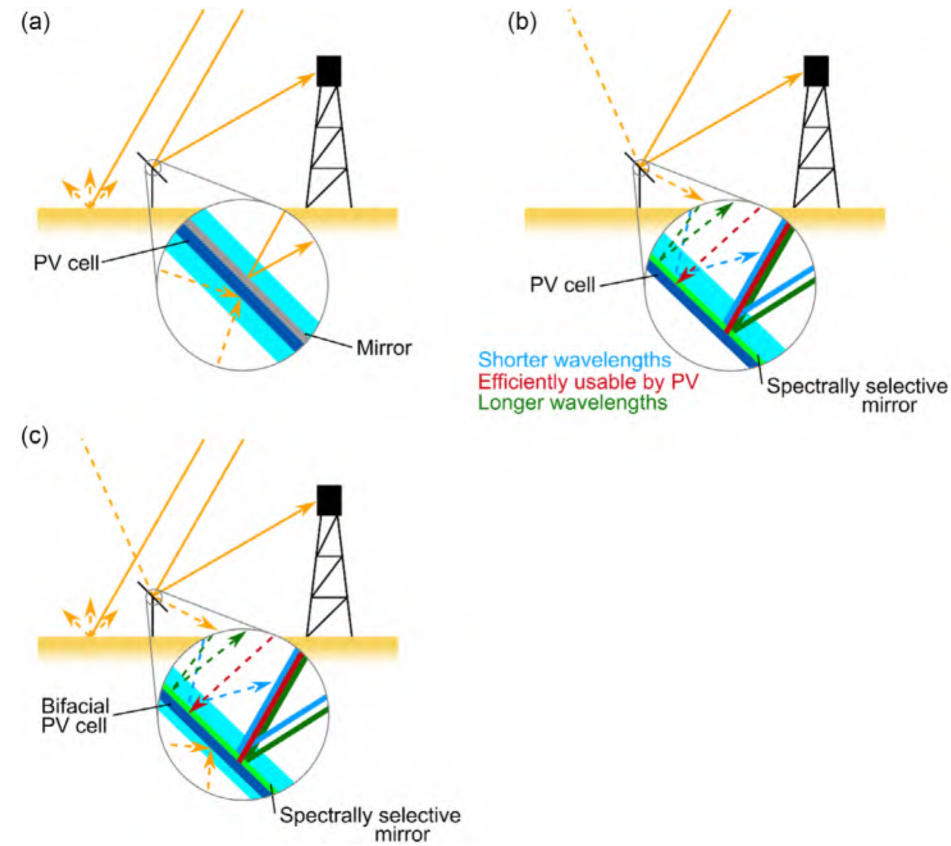

Figure 3. Schematic overview of the three integrated CST/PV hybrid concepts replacing the mirrors: a) Rear-PV, b) PV-Mirror, and c) bifacial PV-Mirror.

also transmitted through the spectrally selective mirrors and can be utilized by the PV cells. When a PV-Mirror is not needed to concentrate radiation, it can be oriented toward the sun.

2.2.3. Bifacial PV-Mirror

Based on the same concept as a PV-Mirror, with a bifacial PV cell rather than a monofacial one, it combines the spectrum splitting of the PV-Mirror with the utilization of the radiation on the backside. When the bifacial PV-Mirror is not needed to concentrate radiation, either the front or back can be oriented toward the sun, whichever is possible and has higher yield.

2.2.4. Spillage-CPV

The fourth concept, Spillage-CPV, is applied in the concentrated part of the system. PV modules for concentrated irradiation (CPV modules) mounted next to the receiver (**Figure 4**) convert the spilled radiation around the receiver into electricity. They utilize III–V semiconductors with a much lower-temperature coefficient than the commonly used silicon and active cooling to be able to convert high radiation fluxes efficiently. The Spillage-CPV is relevant in CRSs with high concentration on the receiver, where the spillage loss can be quite significant. In this concept, also radiation that otherwise would be dumped can be directed onto the CPV cells instead.

2.3. Literature Review

2.3.1. Rear-PV

The Rear-PV, for which the realization in one panel is patented,[3] was modeled for the use in an existing LFC supplying heat for air conditioning of a research building in Cyprus.[4,5] It was calculated that the levelized cost of heat supplied by the LFC could be lowered by around 10% while the electric energy saved for the air conditioning could be more than doubled. In this case, the LFC is only needed if air conditioning of the building is also required, only during part of the year, and only on working days when the building is used. During the remaining dumping time, the mirrors can be flipped over, and the advantage of the Rear-PV is increased.

2.3.2. PV-Mirror and Bifacial PV-Mirror

The concept of the PV-Mirror for the use in CST systems was first studied in 2015.[6] Also, the use of spectrally selective mirrors on top of PV cells to reduce their operating temperature has been investigated.[18–29] Cote et al. modeled the use of spectrally selective mirrors with bifacial PV cells as it is relevant to the bifacial PV-Mirror.[29] Yu et al. discussed the use of the PV-Mirror in a decoupled PV–PV tandem and in CSP applications.[6] For the use in the PV–PV tandem, i.e., a CPV system with PV-Mirrors instead of conventional solar mirrors, higher efficiencies are predicted than for a monolithic PV–PV tandem operating under concentrated radiation, since diffuse radiation can also be utilized with the PV-Mirror. Increases in efficiency are also predicted for use in CSP applications while maintaining dispatchability. Very optimistic laboratory efficiency under standard conditions is assumed for PV modules.

Yu et al. evaluated different methods to realize the spectrally selective mirror.[7] They consist in depositing a dielectric layer stack on the PV cell or on the cover glass and the use of commercially available foil. Furthermore, Yu et al. discussed the potential to lower the LCOE from CSP plants equipped with the PV-Mirror by over 15%.[8] However, LCOEs of CSP electricity and PV electricity have to be treated separately as the cost of dispatchability differs for the two of them.[2] In 2019, Yu et al. experimentally investigated the use of the PV-Mirror not for CST applications but to form a tandem with another PV module.[9] System efficiency of 29.6% is reported.

Ziyati et al. developed a model for using the PV-Mirror in CRSs.[10,11]

Liew et al. modeled the use of the PV-Mirror in a collector for supplying heat for domestic requirements.[30]

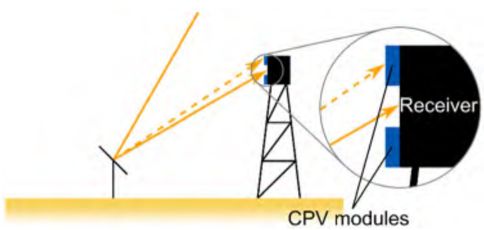

Figure 4. Schematic depiction of the Spillage-CPV.

2.3.3. Spillage-CPV

Das et al. and Ho et al. determined the break-even cost of Spillage-CPV.[12,13] It was calculated that the Spillage-CPV achieves the same LCOE as stand-alone PV at concentration factors of the spillage of about 100.[13] For increasing concentration factor, the LCOE decreases.

3. Technological Discussion

3.1. Realization and Technological Aspects of Solar Mirrors

For reasons of lifetime of the mirrors, they are usually realized as second surface mirrors, i.e., the reflective layer is on the backside of glass. The common design of conventional solar mirrors is schematically depicted in **Figure 5**. To protect the reflective silver layer, a copper layer is applied with further coatings of varnish. The copper increases the adhesion of the varnish layers, blocks the ultraviolet (UV) radiation the silver transmits to protect the varnish, and prevents corrosion of the silver by acting as a sacrificial anode.

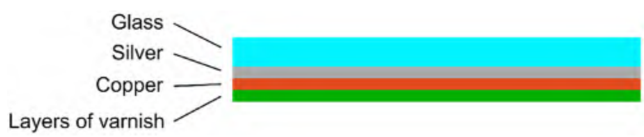

Figure 5. Schematic of the layers of a conventional solar mirror (not to scale).

The protection on the back can also be achieved by laminating glass, metal, or compound material on the backside instead of layers of varnish. This increases the corrosion protection. Due to the higher cost, laminated mirrors are not commonly applied.

The required mechanical resistance of the mirror is provided by the glass itself, commonly 3–4 mm thick. Laminated mirrors with thin front glass (around 1 mm) achieve the shape from a stable substrate or sandwich type panel. Thin glass has the advantage of less absorption in the glass and thus higher reflectance of the mirror. An increase of around 1% can be expected.[31]

3.2. Realization and Technological Aspects of PV

PV modules are typically made by laminating PV cells between glass on the front side and polyvinyl fluoride (PVF) foil on the backside. The most common encapsulant is ethylene-vinyl acetate (EVA) (**Figure 6**).

For bifacial PV modules, the PVF foil is replaced with a transparent back cover. Glass is the industry standard. This requires to change the encapsulant, as increased degradation of EVA is observed in glass–glass modules.[32]

Degradation processes in PV modules are mainly thermally activated and due to UV radiation. These degradation processes lead to decreases in power output of up to 1–2 percent per year.[33]

3.3. Technological Aspects and Possible Realization of the Four Concepts

3.3.1. Rear-PV

This work proposes realizing the Rear-PV based on the design of PV modules. To make the Rear-PV, the PVF foil is replaced with a mirror. Glass is proposed as cover sheet. As described earlier, for glass–glass modules, an encapsulant other than EVA has to be used. However, in this case, due to the mirror on top of the system, much less light hits the encapsulant such that EVA still might be viable.

The design in **Figure 7** has advantages over the solution of just mounting PV modules on the back of the mirrors. First, material consumption and weight are reduced. To maintain the same mechanical properties as a conventional solar mirror, it is assumed that the cover glass of the PV and the glass used for the mirror can be thinner than in the respective stand-alone applications. One option would be to use the thinnest glass possible for the mirror to achieve maximum reflectance and choose the thickness of the glass for the PV side so that it provides the desired mechanical properties. Varnish protection layers on the back of the mirror are not needed because the silver layer is protected against corrosion by the lamination. The copper layer could still be useful to protect the encapsulant from UV radiation. The processes needed for the production of the proposed design of the Rear-PV are well known from the production of glass–glass PV modules and mirrors. If the protecting varnish on the back of the silver of the mirror is dropped, oxidation of the silver has to be prevented before lamination.

The Rear-PV in the proposed configuration slightly increases the reflectance of the mirrors, no extensive adaptions of the CST system are required. However, CST applications can be redesigned regarding the balance of the different loss channels. The aperture area can be more oversized to allow higher receiver utilization as during the increased periods of dumping the PV can be used to generate electricity. Furthermore, higher GCRs are possible as blocked radiation can be utilized, while blocking leads to inhomogeneous illumination of the PV, which has to be considered in aiming strategies and the interconnection of the PV cells. Lastly, the zone in which CST applications can be operated economically can be extended to regions with lower average DNI, as the Rear-PV converts the global irradiation.

The feasibility of Rear-PV could be increased by artificially increasing the ground albedo or, respectively, choosing the site according to the ground albedo.

One issue with implementing Rear-PV is inhomogeneous illumination of the backside of the mirrors, because of shadowing due to the supporting structure and blocked radiation. To mitigate the negative effect due to the blocked radiation the cells should be wired accordingly and the aiming strategies can be adapted. Apart from the blocked radiation in normal operation, the light hitting the back of the mirrors is diffuse, as it is sunlight scattered on the ground; therefore, the negative influence of the shadowing due to the supporting structure is reduced. Furthermore, in a CRS the mirrors are two-axis tracked. That means when mirrors are flipped backside up, the shadow of the supporting structure is all the time at the same place. These areas could either not be equipped with PV cells, or the cells in these areas could be wired to minimize the negative influence of the partial shading.

Additional to the typical candidates for absorber materials for PV cells for the Rear-PV, low-efficiency materials like amorphous silicon might be feasible: in CST applications, the racking required for the Rear-PV is already in place. To assess the cost of Rear-PV, only the cost of the components themselves are relevant. One of the main drawbacks of low efficiency absorber materials is the fact that required racking costs are high with respect to the generated electricity. This disadvantage is not an issue in the case of the Rear-PV. In addition, thin-film PV generally deals better with shadowing because the individual cells are arranged in stripes rather than tiles.

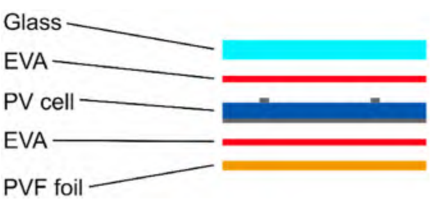

Figure 6. Design of a standard PV module (not to scale).

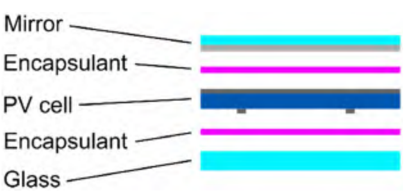

Figure 7. Proposed design of the Rear-PV (not to scale).

3.3.2. PV-Mirror

The PV-Mirror can be produced by providing the glass of PV modules with a spectrally selective layer (**Figure 8**). This can be sputtered, or a commercially available foil can be used. Large-scale sputtering of glass is already established due to, e.g., low emissivity coating for window glass.

In this work, it is proposed to place the spectrally selective layer at the interface of glass and encapsulant to protect it from environmental effects. A placement on the outer surface of the glass would allow for an antireflective effect and possibly increased radiative cooling of the modules.[20,24] The combination with a conventional antireflective coating on the outside of the glass is possible as well.

Yu et al. discussed a further implementation: PV cells with good transmittance of sub-bandgap photons in combination with a back reflector.[6] This option is also studied by Ziyati et al.[10,11] Here the reflection is angle independent. In this work, still the first approach is followed, since it allows the use of all commercially available PV cells. This option has another key advantage: the characteristics of the spectrally selective mirror, and thus the split of the incident spectrum between CST and PV can be adjusted to optimize energy production. The spectrally selective mirror can also be designed to reflect UV light to protect the underlying components.[21]

The spectrally selective mirror reduces the operating temperature of the PV cells. For an ideal sub-bandgap reflector placed on the interface of glass and encapsulant an irradiance-weighted reduction of the annual average operating temperature of 3.8 K is predicted by simulation,[22] leading to increased efficiency and reduced thermally induced degradation processes. Silverman et al. estimated an increase of the PV lifetime by 26%–200%.[22]

Due to the lower reflectance of the PV-Mirror, the ideal configuration for CST applications using the PV-Mirror could differ significantly from the one with conventional mirrors. It is assumed that the efficiency of CST applications decreases with reduced reflectance of the mirrors: if the reduced reflectance is to be compensated by more aperture area, additional mirrors placed further away from the receiver, resulting in lower optical efficiency. If instead lower concentration factor is designed at the receiver, the efficiency also decreases. Therefore, the PV-Mirror might be unsuitable for some CST applications, especially those requiring very high concentration factors, or different designs of the spectrally selective mirror must be found for different applications.

Since the PV-Mirror, like the Rear-PV, can generate power during dumping periods, the aperture area can be oversized to allow for better receiver utilization. Since the PV-Mirror can also convert some of the diffuse radiation and generate power with the PV during low DNI, it potentially expands the zone in which CST applications can be operated economically to regions with lower average DNI.

As in the case of the Rear-PV, the use of thin-film PV technology, such as amorphous silicon, could be feasible for the PV-Mirror. Only additional costs for the PV layers are incurred, racking and glass are already available. Analyses must verify if the PV electricity can outweigh the negative effects of reducing the reflectance of the mirrors.

3.3.3. Bifacial PV-Mirror

The bifacial PV-Mirror can be fabricated analogously to the PV-Mirror, but starting from a bifacial PV module (**Figure 9**). The thickness of the cover glass can be chosen as thin as possible to enable high reflectance while the mechanical stability is given by the back-glass.

The bifacial PV-Mirror has the same advantages as the PV-Mirror: protection of the materials against UV radiation and reduced heating of the PV cells, and thus overall reduced degradation and increased efficiency. Cote et al. calculated a reduction of the cell temperature of 2.7 K under front side only AM1.5 illumination for bifacial PV cells with ideal spectrally selective mirrors on top.[29] As with the PV-Mirror the reflectance is lower than for standard solar mirrors, so that the configuration of the CST application should be adapted accordingly. Whenever the full aperture area is not needed for concentrating sunlight, either front or backside can be oriented toward the sun to generate PV power, depending on technical feasibility. Again, oversizing the aperture area is reasonable, and CST technologies can potentially be extended to regions with lower average DNI.

3.3.4. Spillage-CPV

For the Spillage-CPV, commercially available CPV cells as the AZUR SPACE 3C44 can be used.[34] They require an effective cooling system and a cover to protect them from dust.

As this front cover receives high radiation flux, it is expected to require regular cleaning to avoid soiling-induced hot spots. Automated cleaning equipment will be advantageous.

Like the other concepts, the Spillage-CPV can also convert excess solar energy minimizing dumping loss. Oversizing of the aperture area is reasonable. In contrast to the other concepts Spillage-CPV does not convert diffuse light.

All of the concepts produce electricity at a power profile differing from stand-alone PV, e.g., the Rear-PV at some times faces the ground and on other times the sun.

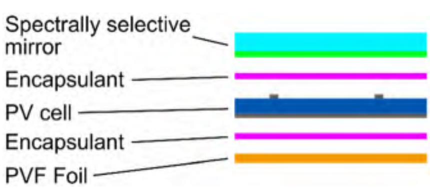

Figure 8. Proposed design of the PV-Mirror (not to scale).

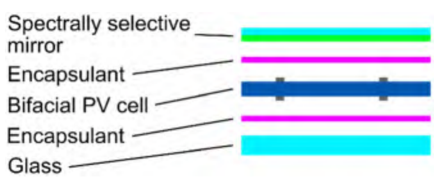

Figure 9. Proposed design of the bifacial PV-Mirror (not to scale).

4. Energy Production

The goal of this chapter is to estimate and compare the CSP and PV production of CSP plants using the different hybrid concepts. The calculations made are not meant to give precise global averages but rather an approximation of the expected yield and a first reference point to compare them. Energy production is described in this section only for CSP, as only for CSP sufficient information regarding energy production and cost is available.

CSP plant design would optimally be adapted for the use of the hybrid concepts, as described earlier, but such optimization goes beyond state of the art and the scope of this work. It is assumed that power plant design remains unchanged for the hybridization. Only CRSs are investigated to include the Spillage-CPV concept.

To quantify the energy production of concept i, the relative hybrid CSP production r_i and the relative hybrid PV production a_i are defined as

$$r_i = \frac{E^i_{\mathrm{CSP}}}{E_{\mathrm{CSP}}} \quad (1)$$

$$a_i = \frac{E^i_{\mathrm{PV}}}{E_{\mathrm{CSP}}} \quad (2)$$

Annual energy production of the non-hybridized CRS power plant is denoted as E_{CSP}. Annual energy production of the CSP plant using concept i in the same configuration as in the non-hybridized case is denoted as E^i_{CSP}. The PV energy production of concept i is denoted by E^i_{PV}.

Crystalline silicon is assumed as material of the PV. For the Spillage-CPV, multi-junction III/IV-cells (e.g., GaInP/GaInAs/Ge of the AZUR SPACE 3C44 cells) with high-efficiency and lower-temperature coefficient are assumed.

4.1. Rear-PV

The reflectance of the thin-glass mirrors is slightly higher than for standard solar mirrors, increasing the radiation flux at the receiver. This is assumed to enhance the annual CSP yield by 2%, considering reduced relative system heat losses, such that $r_{\mathrm{RPV}} = 102\%$. The receiver has to be scaled up accordingly.

For the estimation of the hybrid PV production a_{RPV}, the parameter b_{RPV} compares annual Rear-PV energy production to a fixed-tilt stand-alone PV power plant with same aperture size:

$$b_{\mathrm{RPV}} = \frac{E^{\mathrm{RPV}}_{\mathrm{PV}}}{E_{\mathrm{PV}}} \quad (3)$$

Here, E_{PV} is the annual amount of energy the stand-alone reference PV power plant produces. The whole back of the mirrors is assumed to be equipped with PV cells.

The PV energy production of the Rear-PV can be separated into three different categories of sources of radiation on the back, denoted by the subscript j, that make up a fraction of the total time during which CSP operation in principle would be possible t_j: first, normal CSP operation, denoted by subscript 1; second, times when DNI is too low for CSP operation, denoted by subscript 2; and third, times when CSP operation is interrupted for other reasons (maintenance [during t_{M}], dumping [during t_{D}]) denoted by the subscript 3: $t_3 = t_{\mathrm{M}} + t_{\mathrm{D}}$

$$b_{\mathrm{RPV}} = (1 - t_2 - t_3) b_{\mathrm{RPV},1} + t_2 b_{\mathrm{RPV},2} + t_3 b_{\mathrm{RPV},3} \quad (4)$$

$$b_{\mathrm{RPV},1} = \frac{E^{\mathrm{RPV}}_{\mathrm{PV},1}}{E_{\mathrm{PV},1}} \quad (5)$$

$$b_{\mathrm{RPV},2} = \frac{E^{\mathrm{RPV}}_{\mathrm{PV},2}}{E_{\mathrm{PV},2}} \quad (6)$$

$$b_{\mathrm{RPV},3} = \frac{E^{\mathrm{RPV}}_{\mathrm{PV},3}}{E_{\mathrm{PV},3}} \quad (7)$$

The $E^{\mathrm{RPV}}_{\mathrm{PV,j}}$ and $E_{\mathrm{PV,j}}$ denote hybrid and stand-alone PV production during t_j. The values of the parameters assumed for the calculation of Rear-PV production b_{RPV} are summarized in **Table 1**.

The $b_{\mathrm{RPV},i}$ are the ratio of radiation energy on the PV of the Rear-PV to the energy on the PV modules of the reference PV power plant, $b_{\mathrm{RPV},1}$ is estimated using technical data for bifacial PV modules. The ratio of the energy on the backside to the energy on the front g can be calculated to 9% independently of the tracking type (global average ±60° latitude).[35] A variety of factors such as ground albedo, GCR, orientation of the modules, and latitude affect g. For all kinds of PV power plants, the backside ratio g is assumed to be 4%–15% independent of the tracking type for ±60° latitude.[35–37] The tracking of the mirrors is assumed to have no effect on the radiation on their back. PV contribution during CSP operation is the sum of energy from diffuse radiation and blocking:

$$b_{\mathrm{RPV},1} = g + p_{\mathrm{b}} \quad (8)$$

During times without CSP operation, the PV modules can be tracked in two axes:

$$b_{\mathrm{RPV},2} = p_{\mathrm{c}} p_{2\mathrm{T}} \quad (9)$$

$$b_{\mathrm{RPV},3} = p_{2\mathrm{T}} \quad (10)$$

Table 1. Parameter assumptions of the Rear-PV production.

Parameter	Assumption
Fraction of time with DNI too low for CSP operation (t_2)	15%
Fraction of annual CSP production lost due to maintenance (t_{M})	3.5%
Fraction of incident energy subject to dumping (t_{D})	2.5%
Backside ratio: the ratio of the radiation energy on the back of bifacial PV modules to the radiation energy on their front (g)[35–37]	9% on global average with a range of 4%–15%
Blocked fraction of incident energy (on rear side of another solar mirror) (p_{b})	1%
Fraction of average GHI during times when DNI is too low for CSP operation (p_{c})	20%
Ratio of annual yield of two-axis-tracked PV system to yield of PV system with fixed tilt, global average for ±60° latitude[35] ($p_{2\mathrm{T}}$)	1.31

$$b_{\mathrm{RPV}} = (1 - t_2 - t_{\mathrm{M}} - t_{\mathrm{D}}) \cdot (g + p_{\mathrm{b}}) + t_2 p_{\mathrm{c}} p_{2\mathrm{T}} + (t_{\mathrm{M}} + t_{\mathrm{D}}) p_{2\mathrm{T}} \tag{11}$$

The resulting ratio of energy from the PV part to the reference PV system b_{RPV} is 20% as global average, with a range from 16% to 24% for g from 4% to 15%.

The hybrid PV production a_{RPV} is related to b_{RPV} by the ratio of CSP and PV efficiencies η_{CSP} and η_{PV} (ρ):

$$a_{\mathrm{RPV}} = \frac{b_{\mathrm{RPV}}}{\rho} \tag{12}$$

$$\rho = \frac{\eta_{\mathrm{CSP}}}{\eta_{\mathrm{PV}}} \tag{13}$$

CSP efficiency is usually referred to annual DNI while PV efficiency is referred to annual global horizontal irradiance (GHI). Annual CSP efficiency of 14%[38–40] and annual PV efficiency for fixed tilt installation of 16%[41] are assumed. The ratio of the annual DNI to annual GHI at suitable CSP locations is assumed to be 1.3:[42]

$$\rho = \frac{14\%}{16\%} \cdot 1.3 \approx 1.1 \tag{14}$$

The resulting hybrid PV production a_{RPV} is 17% as global average, with a range from 14% to 21% for g from 4% to 15%.

4.2. PV-Mirror

For the PV-Mirror, the transmission and reflection characteristics of the spectrally selective mirror determine the relative hybrid CSP and PV production, r_{PVM} and a_{PVM}. Mirror characteristics will have to be optimized in terms of yield or LCOE.

Ziyati et al. simulated the use of the PV-Mirror in a CRS.[10] The simplest way of splitting the spectrum is discussed: the sub-bandgap light is reflected to the thermal receiver while all other light is transmitted to the PV. Gallium arsenide (GaAs) PV with a back reflector is simulated as PV-Mirror. The simulation is available with the efficiency of the GaAs PV normalized to the efficiency of silicon PV. It calculated a hybrid CSP production of $r_{\mathrm{PVM}} = 36\%$ and a hybrid PV production of $a_{\mathrm{PVM}} = 93\%$.

It is discussed whether they hold also for silicon PV with spectrally selective mirrors, as proposed in this work. There are two main differences with silicon cells: the bandgap is smaller than for GaAs (Si: 1.1 eV, GaAs: 1.4 eV), and transmittance of the spectrally selective mirror depends on the angle of incidence.

The smaller bandgap means that at normal incidence only part of the super-bandgap radiation, defined by, e.g., a transmission window, has to be used to get the same outputs from PV and CSP as in the simulation of Ziyati et al. However, the efficiency of PV for super-bandgap light is not constant. Therefore, the part of the super-bandgap light transmitted to the PV can be chosen in such a way that the PV can use it with an increased average efficiency compared to the simulation of Ziyati et al. That increases a_{PVM} for silicon PV.

For non-normal incidence, the transmission window shifts to shorter wavelengths.[7] That is expected to decrease the power inside the window, shifting the share between CSP and PV toward CSP. Furthermore, this decreases the average efficiency inside the transmission window, increasing the hybrid CSP production r_{PVM} and a decreasing the hybrid PV production a_{PVM}.

4.3. Bifacial PV-Mirror

For the bifacial PV-Mirror, the same hybrid CSP production as for the PV-Mirror, $r_{\mathrm{BPVM}} = 36\%$, is as assumed. For determining the hybrid PV production a_{BPVM}, the additional energy produced from radiation energy hitting the back of the mirrors during normal operation is added. According to the assumptions made for the Rear-PV and assuming a bifaciality (ratio of efficiency on front to efficiency on back) of 0.8, $a_{\mathrm{BPVM}} = a_{\mathrm{PVM}} + b_{\mathrm{RPV},1} \cdot 0.8 \cdot \rho^{-1}$ results to 100% on global average, with a range from 97% to 104% for g from 4% to 15%.

4.4. Spillage-CPV

The Spillage-CPV has the same CSP production as the reference CSP plant ($r_{\mathrm{SCPV}} = 1$).

The relative hybrid PV production a_{SCPV} is essentially determined by the spillage fraction of concentrated radiation. A share of spillage γ is assumed to range between 5% and 30%. Low values are reported in commercial CSP plants and high values for high-temperature receivers. Additional 2.5% of the total energy from dumping can be reflected onto the CPV cells.

The efficiency of the CSP thermodynamic cycle (power block) η_{CSP} is assumed to be 40%.[43,44] While cell efficiency of the AZUR SPACE 3C44 is ≈40% as well, the module efficiency η_{CPV} is assumed to be 32%.[45] The resulting hybrid PV production from the CPV $a_{\mathrm{SCPV}} = \left(0.025 + \frac{\gamma}{1-\gamma}\right) \cdot \frac{\eta_{\mathrm{CPV}}}{\eta_{\mathrm{CSP}}}$ is 8%–36% for the amount of captured spilled radiation energy γ ranging from 5% to 30%.

All assumptions of this section are summarized in **Table 2**.

4.5. Discussion

In **Figure 10**, the CSP and PV hybrid energy production of the different concepts is summarized and compared to the reference system, the CSP plant, assumed with 14% annual efficiency. In green, the CSP production r_i, and, in blue, the hybrid PV production a_i are shown. The light blue areas mark the range of the hybrid PV production depending on input assumptions.

Considering the range of the PV production, the bifacial PV-Mirror yields the highest amount of additional energy of 40%, followed by Spillage-CPV (up to 36%, lower end 8%, depending on the amount of technically available spillage around the receiver) and PV-Mirror (29%), while Rear-PV (23%) gives the lowest amount of additional energy.

The range of the amount of energy generated by the PV of the hybrid concepts in the case of Rear-PV and bifacial PV-Mirror is due to the uncertainty of the radiation flux hitting the backside of the mirrors. For several reasons, it can be assumed that the actual radiation energy hitting the backside of the mirrors is higher than the global average of the radiation flux hitting the backside of bifacial PV modules: the ground albedo at typical CST sites is increased compared to the global average. This increases the radiation flux onto the backside of the mirrors.[46]

Table 2. Summary of all assumptions of the section "Energy production".

Parameter	Assumption
Fraction of time with DNI too low for CSP operation (t_2)	15%
Fraction of annual CSP production lost due to maintenance (t_M)	3.5%
Fraction of incident energy subject to dumping (t_D)	2.5%
Backside ratio: the ratio of the radiation energy on the back of bifacial PV modules to the radiation energy on their front (g)[35–37]	9% on global average with a range of 4%–15%
Blocked fraction of incident energy (on rear side of another solar mirror) (p_b)	1%
Fraction of average GHI during times when DNI is too low for CSP operation (p_c)	20%
Ratio of annual yield of two-axis tracked PV system to yield of PV system with fixed tilt, global average for ±60° latitude[35] (p_{2T})	1.31
Annual CSP efficiency (η_{CSP})[38–40]	14%
Annual PV efficiency for fixed tilt installation (η_{PV})[41]	16%
Ratio of the annual DNI to annual GHI at suitable CSP locations[42]	1.3
Share of spillage (γ)	5%–30%
CSP power block efficiency (η_{CSP})	40%
CPV module efficiency (η_{CPV})[45]	32%

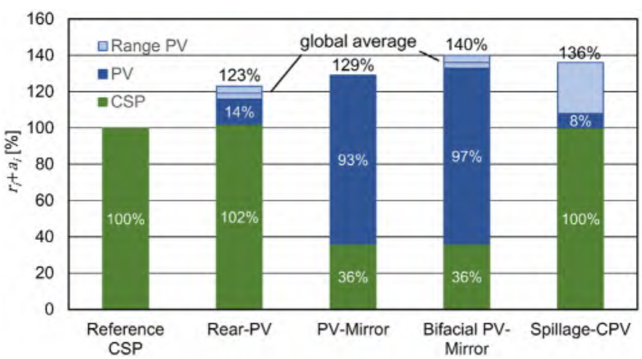

Figure 10. Comparison of the energy production of the integrated hybrid concepts to the reference CSP plant (14% efficiency).

Furthermore, the GCR in CST applications is lower than in PV power plants (e.g., CSP: Gemasolar project 0.21,[39] PV: 0.35 assumed in Pelaez et al.[36]). This also leads to an increase of the radiation flux to the backside of the mirrors.[46] Unlike PV modules, the surrounding mirrors are highly reflective such that they reflect a significant amount of diffuse radiation from the sky onto the back of the mirrors.

As mentioned earlier, the values for the PV-Mirror and the bifacial PV-Mirror depend on the characteristics of the spectrally selective mirror used. The values shown here represent only one possible configuration. For example, it would be possible to reflect much more light for the CST application, which might be necessary especially for high-temperature applications, as decreased reflectance lowers the maximum achievable concentration factor.

The CRS simulated by Ziyati et al.[10] was located at Targassonne, France, a mediocre CSP location in terms of annual DNI, where the diffuse fraction of the incident radiation is higher than on more suitable CSP locations.[11] For that reason, it is assumed that the PV-Mirror can achieve better results there than at the more suitable locations as it is able to convert a fraction of the diffuse irradiation.

For all concepts, as described earlier, further improvements in energy production are possible, mainly through optimization of power plant configuration. As the reflectance of the mirrors in the case of PV-Mirror and bifacial PV-Mirror is strongly decreased compared to standard solar mirrors, proper optimization of heliostat field size is especially important for these concepts.

5. Cost Considerations

The following cost calculations are basic conceptional considerations regarding the economic aspects of the four technical concepts to clarify relevance of further research.

It is assumed that in an ideal energy mix, a certain proportion of the required energy would be generated by CST technologies and a certain proportion by PV. Cost data is mainly available for CSP as representative for CST. Only CRSs are used to include the Spillage-CPV.

It is assumed that implementing hybrid concepts must not change the amounts of energy generated by CSP and PV. The effect of the hybrid CSP production modifying CSP production requires that the CSP capacity has to be scaled accordingly. Due to the hybrid PV production some stand-alone PV capacity can be saved. To compare the concepts the change in investment cost resulting from scaling of the CSP capacity and the saving of stand-alone PV capacity are evaluated.

For the whole CPV system good estimates for the cost of the required components are available.[45] For the Rear-PV, the PV-Mirror, and bifacial PV-Mirror, the cost of the respective components are unknown. To achieve economic numbers, a criterion is formulated for the maximum cost of each of the concepts that would lead to reduced total cost. In the first step, the change in investment cost due to the scaling of the CSP capacity is calculated. As described earlier, the ideal power plant configuration with modified reflectance is not known. The extreme cases would be to either change nothing in the power plant configuration and therefore have a reduced radiation flux on the receiver, or to increase the heliostat field to maintain the radiation flux on the receiver. The minimum requirement is to scale the overall aperture area. The cost of the remaining parts of the CSP plants is assumed to be constant. This is a simplifying assumption that neglects the fact that the cost of the CSP plant apart from the heliostat field is not proportional to the design point power on the receiver and that the optical efficiency of the heliostat field decreases as its size is increased. Costs for the required cabling of the PV components on the heliostats are neglected as well.

For the Rear-PV, this is a reasonable approximation since the heliostat field size effect is low (r_{RPV} only slightly deviates from 1). For the PV-Mirror and the bifacial PV-Mirror, the deviations will be larger since the aperture area here has to be almost tripled for the assumed configuration of the spectrally selective mirror.

This weakness has to be kept in mind when interpreting the results of this section.

The change in investment cost due to the scaling of the concentrating structure $\Delta_{\mathrm{CSP}}^{i}$ is then calculated as

$$\Delta_{\mathrm{CSP}}^{i} = \left((l_{\mathrm{CSP}} \cdot z_i + m_{\mathrm{CSP}}) \cdot \left(\frac{1}{r_i} - 1 \right) \right) \sigma_{\mathrm{CSP}} \tag{15}$$

with σ_{CSP} being the specific investment cost per annually produced energy for the CSP system, l_{CSP} being the fraction of σ_{CSP} that is spent for only the mirrors, m_{CSP} being the fraction of σ_{CSP} that is proportional to the aperture area excluding the mirrors, and z_i being the ratio of the cost of the hybrid component per aperture area to the cost of conventional mirrors per aperture area for the component of the concept i.

The investment cost of stand-alone PV saved due to the PV electricity produced by the hybrid concept i (Δ_{PV}^{i}) is calculated as

$$\Delta_{\mathrm{PV}}^{i} = \frac{a_i}{r_i} \sigma_{\mathrm{PV}} \tag{16}$$

with the specific investment cost per annually produced energy of the stand-alone PV power plant σ_{PV}. As described earlier, the hybrid concepts produce electricity at a power profile differing from stand-alone PV. The corresponding change of the composition of the mix of energies is neglected.

The condition for a decrease of the investment cost is $\Delta_{\mathrm{PV}}^{i} - \Delta_{\mathrm{CSP}}^{i} > 0$ from which it follows for the cost ratio z_i:

$$z_i < \left(\frac{a_i}{r_i} \frac{\sigma_{\mathrm{PV}}}{\sigma_{\mathrm{CSP}}} + m_{\mathrm{CSP}} \left(1 - \frac{1}{r_i} \right) \right) \frac{r_i}{l_{\mathrm{CSP}}} + r_i \tag{17}$$

The parameters used to calculate the limit for the cost ratio z_i are shown in **Table 3**. The value of the ratio of the investment cost of PV and CSP $\frac{\sigma_{\mathrm{PV}}}{\sigma_{\mathrm{CSP}}}$ is calculated based on *Renewable Power Generation Costs in 2021* taking into account the capacity factors of PV and CSP.[1] There also a value for $m_{\mathrm{CSP}} + l_{\mathrm{CSP}}$ can be found. To calculate the values of m_{CSP} and l_{CSP} from this, the ratio of those two parameters was taken from Dieckmann et al.:[17] $\frac{m_{\mathrm{CSP}}}{l_{\mathrm{CSP}}} = 5.5$.

With this, the upper limit of the cost ratio z_i to reduce the costs can be calculated (**Table 4**).

The costs of the components required for the CPV system for the Spillage-CPV are summarized in **Table 5**.

The investment cost per power for the modules can be calculated from their specific cost with the efficiency of the modules η_{CPV} and the spillage radiation flux F. The required investment cost for the cooling of the system can be calculated using the efficiency of the modules. It is for the total specific investment cost for the Spillage-CPV σ_{SCPV}:

$$\sigma_{\mathrm{SCPV}} = \left(\sigma_{\mathrm{SCPV}}^{\mathrm{Inverter}} + \sigma_{\mathrm{SCPV}}^{\mathrm{Switchgear}} + \sigma_{\mathrm{SCPV}}^{\mathrm{Cooling}} \cdot \frac{1 - \eta_{\mathrm{CPV}}}{\eta_{\mathrm{CPV}}} + \frac{\sigma_{\mathrm{SCPV}}^{\mathrm{CPV}}}{F \cdot \eta_{\mathrm{CPV}}} \right) \cdot (1 + \mathrm{BoP}) \tag{18}$$

The average investment cost of utility-scale PV projects in 2021 was $\sigma_{\mathrm{PV}} = 883\ \$\mathrm{kW}^{-1}$,[1] and the assumed module efficiency of the CPV is 32% as described earlier. The break-even with the investment cost of the stand-alone PV ($\sigma_{\mathrm{SCPV}} = \sigma_{\mathrm{PV}}$) is reached for spillage radiation fluxes of $F \approx 350\ \mathrm{kWm}^{-2}$ at peak.

All assumptions of this section are summarized in **Table 6**.

Table 3. Cost data used for calculating the limit for the cost of the hybrid components.

Parameter	CRS
Ratio of the investment cost of PV and CSP ($\frac{\sigma_{\mathrm{CSP}}}{\sigma_{\mathrm{PV}}}$)[1]	2.72
Percentage of cost of concentrating structure excluding mirrors of specific investment cost per annually produced energy of CSP systems (m_{CSP})[1,17]	0.24
Percentage of cost of solar mirrors of specific investment cost per annually produced energy of CSP systems (l_{CSP})[1,17]	0.04

Table 4. Upper limit of the cost of the hybrid concepts for CRSs.

	Rear-PV	PV-Mirror	Bifacial PV-Mirror
Upper limit of z_i	2.6 with a range of 2.3–3.0	4.8	5.4 with a range of 5.1–5.7

Table 5. Cost of the components required for the CPV system assuming an exchange rate from Euro to USD of about 1.08.[45]

Parameter	Value
Specific cost CPV modules ($\sigma_{\mathrm{SCPV}}^{\mathrm{CPV}}$)	48 000 $\$\mathrm{m}^{-2}$
Specific cost cooling system including installation ($\sigma_{\mathrm{SCPV}}^{\mathrm{Cooling}}$)	77 $\$\mathrm{kW_{thermal}}^{-1}$
Specific cost inverter including installation ($\sigma_{\mathrm{SCPV}}^{\mathrm{Inverter}}$)	81 $\$\mathrm{kW_{electric}}^{-1}$
Specific cost high-voltage switchgear including installation ($\sigma_{\mathrm{SCPV}}^{\mathrm{Switchgear}}$)	63 $\$\mathrm{kW_{electric}}^{-1}$
Balance of plant CPV (BoP)	20%

5.1. Discussion

To determine whether the limits for the cost of the hybrid concepts can be realistically met, the costs of the components are estimated.

In 2021, the cost of PV modules and inverters was 380 $\$\mathrm{kW}^{-1}$.[1] Assuming a module efficiency of 21%,[47] the specific module area is 4.8 $\mathrm{m^2kW^{-1}}$, at a cost of 79 $\$\mathrm{m}^{-2}$ for modules including inverters.

For flat CSP mirrors, a cost of 17 $\$\mathrm{m}^{-2}$ is assumed.[17]

For the Rear-PV produced by lamination as described earlier, the mirror and the PV modules with inverters are needed. As an approximation for the real cost, the sum of PV and mirror of 96 $\$\mathrm{m}^{-2}$ is assumed. That means that the actual value of the cost ratio z_{RPV} will be around $z_{\mathrm{RPV}} \approx \frac{96\ \$/\mathrm{m}^{-2}}{17\ \$/\mathrm{m}^{-2}} = 5.6$. Even with further reductions of the cost with savings of material described earlier, this is expected to be higher than the limit calculated for z_{RPV} according to Table 4.

The PV-Mirror and the bifacial PV-Mirror can be realized by deploying the cover glass of monofacial or bifacial PV modules with a spectrally selective coating. The cost of the PV modules

Table 6. Summary of all assumptions of the section "Cost considerations".

Parameter	Assumption
Ratio of the investment cost of PV and CSP ($\frac{\sigma_{CSP}}{\sigma_{PV}}$) for CRSs[1]	2.72
Percentage of cost of concentrating structure excluding mirrors of specific investment cost per annually produced energy of CSP systems (m_{CSP}) for CRSs[1,17]	0.24
Percentage of cost of solar mirrors of specific investment cost per annually produced energy of CSP systems (l_{CSP}) for CRSs[1,17]	0.04
Specific cost CPV modules (σ_{SCPV}^{CPV}) assuming an exchange rate from Euro to USD of about 1.08[45]	48 000 $\$m^{-2}$
Specific cost cooling system including installation ($\sigma_{SCPV}^{Cooling}$) assuming an exchange rate from Euro to USD of about 1.08	77 $\$kW_{thermal}^{-1}$
Specific cost inverter including installation ($\sigma_{SCPV}^{Inverter}$) assuming an exchange rate from Euro to USD of about 1.08[45]	81 $\$kW_{electric}^{-1}$
Specific cost high-voltage switchgear including installation ($\sigma_{SCPV}^{Switchgear}$) assuming an exchange rate from Euro to USD of about 1.08[45]	63 $\$kW_{electric}^{-1}$
Balance of plant (BoP) CPV[45]	20%

plus inverters is taken as a lower bound since the cost of the spectrally selective coating is not available. Based on 79 $\$m^{-2}$ for monofacial modules plus inverters, the cost ratio is $z_{PVM} > \frac{79\ \$/m^{-2}}{17\ \$/m^{-2}} = 4.6$. For bifacial modules, this cost is assumed 10% higher,[48] resulting in the cost ratio $z_{BPVM} > 5.1$. This means that the margin for the spectrally selective coating is for the PV-Mirror $0.2 \cdot 17\ \$/m^{-2} \approx 3.4\ \$/m^{-2}$ and analogously 5.1 $\$m^{-2}$ on global average with a range from 0 to 10.2 $\$m^{-2}$ for the bifacial PV-Mirror. The expected increase in lifetime of the PV cells of the PV-Mirror concepts due to less irradiance is expected to lead to further reductions of the LCOE.

The fact that only spillage with peak radiation flux of over roughly 350 kWm^{-2} can be converted cost-effectively, limits the Spillage-CPV production and thus decreases its relative energy production a_{SCPV}. Such high values of spillage radiation flux are only available in high-temperature receivers.

From this discussion, it is derived that PV-Mirror and bifacial PV-Mirror can become economically feasible concepts. The aforementioned assumption that only the CSP aperture area has to be scaled for these concepts neglects additional cost of the modified CSP part. These additional costs are smallest in low-concentrating systems. On the technical side, the spectral properties of the spectrally selective mirror have to be optimized.

The result for the Rear-PV concept shows that it will not be feasible in existing CSP designs. The Spillage-CPV will bring the biggest economic advantage in high-temperature CST systems where the amount and the concentration of the spillage are highest.

All the concepts bear the chance of optimizing the CSP design to account for the changes of mirror reflectance and to better utilize the strengths of the concepts to exploit loss channels of CST, even at a level to possibly bring all of the concepts to become techno-economically viable options.

6. Conclusion

The implementation of Rear-PV, PV-Mirror, bifacial PV-Mirror, and Spillage-CPV in a CSP tower plant leads to an additional energy yield as high as 23%, 29%, 40%, and 36%, respectively, on the same mirror aperture size. This is achieved by utilizing unused potentials of stand-alone CST systems and PV. The maximum allowable costs per aperture are for the concepts of the Rear-PV, PV-Mirror, and bifacial PV-Mirror can be 3.0, 4.8, and 5.7 times the cost of conventional mirrors. In the case of the Spillage-CPV, a break-even of LCOE with stand-alone PV can be achieved if it is only installed in areas with spillage radiation flux exceeding ≈140 kWm^{-2} at peak if operation and maintenance cost do not differ from those of stand-alone PV.

The technological readiness level of the four hybrid concepts differs significantly. The Spillage-CPV is most advanced, as such cells are available and already in use in CPV power plants. The study showed that when the spillage flux threshold of ≈350 kWm^{-2} peak is exceeded around the CST receiver the Spillage-CPV is expected to generate electricity at lower investment cost than stand-alone PV. Further optimized power plant configuration would fully exploit the CPV cells.

For the use in existing types of CST configurations, the Rear-PV does not appear to be economically feasible because of the low cost-performance ratio. Modified solar field configurations might be realized. Being able to utilize blocked radiation, it can be of interest in locations with limited ground area, such as on roofs, where increasing the albedo can be useful not only to increase the yield of rear PV but also to reduce the heat-up of the building. Rear-PV should not to be discarded for large-scale CST systems either, typically oversized, enabling for electricity generation during dumping periods.

Both monofacial and bifacial PV-Mirrors are potentially feasible in conventional CST configurations already with the configuration of the spectrally selective mirror investigated in this work. To come to better statements on the economic feasibility of the PV-Mirror concepts, the effect of the reduced reflectance on the CST system efficiency has to be studied more in detail. The bifacial PV-Mirror tends to have lower LCOE, or a larger margin for profits. It opens the option of turning the backside up for power production, if heliostat design allows it. Utilization of blocked radiation is lower than for the Rear-PV, since the spectrally selective mirror is designed to mainly reflect radiation that the PV cannot utilize.

For monofacial and bifacial PV mirrors, the power plant configuration and the properties of the spectrally selective mirror require to be optimized depending on the desired application. Both optimizations influence each other. Even within a certain power plant configuration PV mirrors with different properties of the spectrally selective mirror can be useful. It is expected that with these optimizations either of the PV-Mirrors can be even more advantageous than the ones simulated by Ziyati et al.[10] which have been only modeled in a conventional power plant configuration without considering hybridization.

In the future, the concept of the bifacial PV-Mirror will be investigated as it seems to be promising according to the results of this work. Production of prototypes and various tests are planned.

Symbols

Symbol	Dimension	Explanation
a_i		Relative hybrid PV production of concept i (normalized to reference CST production): ratio of E^i_{PV} to E_{CST}
BoP		Balance of plant CPV
b_{RPV}		Relative hybrid PV production of Rear-PV (normalized to stand-alone PV production): ratio of $E^{\mathrm{RPV}}_{\mathrm{PV}}$ to E_{PV}
$b_{\mathrm{RPV},j}$		Relative hybrid PV production of Rear-PV during time period j (normalized to stand-alone PV production): ratio of $E^{\mathrm{RPV}}_{\mathrm{PV},j}$ to $E_{\mathrm{PV},j}$
E_{CST}	Energy	Reference CST production: annual amount of energy of the reference CST application
E^i_{CST}	Energy	Hybrid CST production under use of concept i: annual amount of energy of a CST application under the use of concept i
E_{PV}	Energy	Stand-alone PV production: annual amount of energy of a stand-alone PV power plant with the same aperture area as the PV of the RPV
$E_{\mathrm{PV},j}$	Energy	Stand-alone PV production during time period j: annual amount of energy of a stand-alone PV power plant with the same aperture area as the PV of the RPV
E^i_{PV}	Energy	Hybrid PV production of concept i: annual amount of PV energy of concept i
$E^{\mathrm{RPV}}_{\mathrm{PV},j}$	Energy	Hybrid PV production of Rear-PV during time period : annual amount of PV energy of the Rear-PV during time period j
F	Power per area	Spillage radiation flux
g		Backside ratio: the ratio of the radiation energy on the back of bifacial PV modules to the radiation energy on their front
i		Subscript for concept
j		Subscript for time period: $j = 1$ for normal CSP operation, $j = 2$ for times when CSP operation is interrupted for other reasons (maintenance, dumping), $j = 3$ for times when DNI is too low for CSP operation
l_{CSP}		Percentage of cost of solar mirrors of specific investment cost per annually produced energy of CSP systems
m_{CSP}		Percentage of cost of concentrating structure excluding mirrors of specific investment cost per annually produced energy of CSP systems
$p_{1\mathrm{T}}$		Ratio of annual yield of single-axis-tracked PV system to annual yield of PV system with fixed tilt
$p_{2\mathrm{T}}$		Ratio of annual yield of two-axis-tracked PV system to annual yield of PV system with fixed tilt
p_{b}		Blocked fraction of incident power (on rear side of another solar mirror)
p_{c}		Fraction of average GHI energy available during times when DNI is too low for CST operation
r_i		Relative hybrid CST production under the use of concept i (normalized to reference CST production): ratio of E^i_{CST} to E_{CST}
t_{D}		Fraction of incident energy that has to be dumped
t_j		Annual fraction of time period j
t_{M}		Fraction of time of maintenance
z_i		Ratio of the cost of the hybrid component per aperture area to the cost of conventional mirrors per aperture area for the component of the concept i
γ		Share of spillage
Δ^i_{CSP}	Cost	Change in investment cost due to the scaling of the concentrating structure for the use of concept i per annually produced CSP energy
Δ^i_{PV}	Cost	Investment cost of stand-alone PV saved due to the PV electricity produced by the hybrid concept i per annually produced CSP energy
η_{CPV}		CPV module efficiency
η_{CSP}		Annual efficiency of CSP with respect to the aperture area and DNI
η_{PV}		Annual efficiency of PV with respect to the aperture area and GHI
ρ		Ratio of η_{CSP} and η_{PV}
σ_{CSP}	Cost per energy	Specific investment cost per annually produced energy of CSP systems
σ_{PV}	Cost per energy	Specific investment cost per annually produced energy of PV systems
σ_{SCPV}	Cost per power	Specific investment cost per peak power Spillage-CPV
$\sigma^{\mathrm{Cooling}}_{\mathrm{SCPV}}$	Cost per power	Specific cost CPV cooling system including installation
$\sigma^{\mathrm{CPV}}_{\mathrm{SCPV}}$	Cost per area	Specific cost CPV modules
$\sigma^{\mathrm{Inverter}}_{\mathrm{SCPV}}$	Cost per power	Specific cost inverter including installation
$\sigma^{\mathrm{Switchgear}}_{\mathrm{SCPV}}$	Cost per power	Specific cost high-voltage switchgear including installation

Acknowledgements

Open Access funding enabled and organized by Projekt DEAL.

Conflict of Interest

The authors declare no conflict of interest.

Data Availability Statement

Data sharing is not applicable to this article as no new data were created or analyzed in this study.

Keywords

concentrating solar powers, concentrating solar thermals, hybrids, photovoltaics (PV)

Received: September 22, 2023
Revised: January 15, 2024
Published online:

[1] IRENA, *Renewable Power Generation Costs in 2021*, International Renewable Energy Agency, Abu Dhabi **2022**.
[2] F. Schöniger, R. Thonig, G. Resch, J. Lilliestam, *Energy Sources, Part B: Econom. Plann. Policy* **2021**, *16*, 55.
[3] M. Röger, F. Sutter, DE102018215657 (A1).
[4] A. C. Montenon, C. Papanicolas, in *Proc. of the 6th Int. Conf. on Renewable Energy Sources & Energy Efficiency*, Nicosia, Cyprus, November **2018**.
[5] A. C. Montenon, C. Papanicolas, *Energies* **2021**, *14*, 131.
[6] Z. J. Yu, K. C. Fisher, B. M. Wheelwright, R. P. Angel, Z. C. Holman, *IEEE J. Photovolt.* **2015**, *5*, 1791.
[7] Z. J. Yu, K. C. Fisher, Z. C. Holman, in *IEEE 42nd Photovoltaic Specialist Conf. (PVSC)*, IEEE, Piscataway, NJ **2015**, pp. 1–4.
[8] K. Fisher, Z. Yu, R. Striling, Z. Holman, *AIP Conf. Proc.* **2017**, *1850*, 20004.
[9] Z. J. Yu, K. C. Fisher, X. Meng, J. J. Hyatt, R. P. Angel, Z. C. Holman, *Prog. Photovolt. Res. Appl.* **2019**, *27*, 469.
[10] D. Ziyati, A. Dollet, G. Flamant, Y. Volut, E. Guillot, A. Vossier, *Appl. Energy* **2021**, *288*, 116644.
[11] D. Ziyati, in *2021 IEEE 48th Photovoltaic Specialists Conf. (PVSC)*, IEEE, Piscataway, NJ **2021**, pp. 2060–2066.
[12] A. K. Das, P. Iñigo, J. D. McGrane, R. J. Terdalkar, M. M. Clark, *J. Renewable Sustainable Energy* **2017**, *9*, 23701.
[13] C. K. Ho, C. O. McPheeters, P. R. Sharps, *AIP Conf. Proc.* **2018**, *2033*, 170006.
[14] N. Hanrieder, S. Wilbert, D. Mancera-Guevara, R. Buck, S. Giuliano, R. Pitz-Paal, *Sol. Energy* **2017**, *152*, 193.
[15] P. Kuntz Falcone, *A Handbook for Solar Central Receiver Design*, Sandia National Lab. (SNL-CA), Livermore, CA **1986**.
[16] A. G. Imenes, D. R. Mills, *Sol. Energy Mater. Sol. Cells* **2004**, *84*, 19.
[17] S. Dieckmann, J. Dersch, S. Giuliano, M. Puppe, E. Lüpfert, K. Hennecke, R. Pitz-Paal, M. Taylor, P. Ralon, *AIP Conf. Proc.* **2017**, *1850*, 160004.
[18] H. Meddeb, M. Götz-Köhler, N. Neugebohrn, U. Banik, N. Osterthun, O. Sergeev, D. Berends, C. Lattyak, K. Gehrke, M. Vehse, *Adv. Energy Mater.* **2022**, *12*, 2200713.
[19] K. Mullaney, G. M. Jones, C. A. Kitchen, D. P. Jones, in *Conf. Record of the Twenty Third IEEE Photovoltaic Specialists Conf.*, IEEE, Piscataway, NJ **1993**, pp. 1363–1368.
[20] W. Li, Y. Shi, K. Chen, L. Zhu, S. Fan, *ACS Photonics* **2017**, *4*, 774.
[21] X. Sun, T. J. Silverman, Z. Zhou, M. R. Khan, P. Bermel, M. A. Alam, *IEEE J. Photovolt.* **2017**, *7*, 566.
[22] T. J. Silverman, M. G. Deceglie, I. Subedi, N. J. Podraza, I. M. Slauch, V. E. Ferry, I. Repins, *IEEE J. Photovolt.* **2018**, *8*, 532.
[23] I. Slauch, M. G. Deceglie, T. J. Silverman, V. E. Ferry, *New Concepts in Solar and Thermal Radiation Conversion and Reliability* (Eds: J. N. Munday, P. Bermel, M. D. Kempe), SPIE, Bellingham, WA **2018**, p. 33.
[24] I. M. Slauch, M. G. Deceglie, T. J. Silverman, V. E. Ferry, *ACS Photonics* **2018**, *5*, 1528.
[25] I. M. Slauch, M. G. Deceglie, T. J. Silverman, V. E. Ferry, in *IEEE 7th World Conf. on Photovoltaic Energy Conversion (WCPEC) (A Joint Conf. of 45th IEEE PVSC, 28th PVSEC & 34th EU PVSEC)*, Waikoloa, HI, June **2018**.
[26] I. M. Slauch, M. G. Deceglie, T. J. Silverman, V. E. Ferry, *ACS Appl. Energy Mater.* **2019**, *2*, 3614.
[27] I. M. Slauch, M. G. Deceglie, T. J. Silverman, V. E. Ferry, in *2019 IEEE 46th Photovoltaic Specialists Conf. (PVSC)*, Chicago, IL, June **2019**.
[28] I. M. Slauch, M. G. Deceglie, T. J. Silverman, V. E. Ferry, *Cell Rep. Phys. Sci.* **2021**, *2*, 100430.
[29] B. M. Cote, I. M. Slauch, M. G. Deceglie, T. J. Silverman, V. E. Ferry, *ACS Appl. Energy Mater.* **2021**, *4*, 5397.
[30] N. J. Y. Liew, Z. Yu, Z. Holman, H.-J. Lee, *J. Renewable Sustainable Energy* **2022**, *14*, 13701.
[31] S. Meyen, E. Lüpfert, A. Fernandez-Garcia, C. Kennedy, in *SolarPACES 2010*, Perpignan, France, September **2010**.
[32] A. P. Patel, A. Sinha, G. Tamizhmani, *IEEE J. Photovolt.* **2020**, *10*, 607.
[33] P. Manganiello, M. Balato, M. Vitelli, *IEEE Trans. Ind. Electron.* **2015**, *62*, 7276.
[34] Datasheet AZUR SPACE 3C44 10x10 m2, **2016**, https://www.azurspace.com/index.php/en/products/products-cpv/cpv-solar-cells.
[35] C. D. Rodríguez-Gallegos, H. Liu, O. Gandhi, J. P. Singh, V. Krishnamurthy, A. Kumar, J. S. Stein, S. Wang, L. Li, T. Reindl, I. M. Peters, *Joule* **2020**, *4*, 1514.
[36] S. A. Pelaez, C. Deline, P. Greenberg, J. S. Stein, R. K. Kostuk, *IEEE J. Photovolt.* **2019**, *9*, 715.
[37] L. Burnham, D. Riley, B. Walker, J. M. Pearce, in *2019 IEEE 46th Photovoltaic Specialists Conf. (PVSC)*, Chicago, IL, June **2019**.
[38] F. Dinter, L. Möller, *AIP Conf. Proc.* **2016**, *1734*, 100005.
[39] M. Romero, J. González-Aguilar, *WIREs Energy Environ.* **2014**, *3*, 42.
[40] Gemasolar Website, https://www.energy.sener/project/gemasolar.
[41] R. Chandel, S. S. Chandel, *Prog. Photovolt. Res. Appl.* **2021**, *30*, 27.
[42] K.-J. Riffelmann, G. Weinrebe, M. Balz, *AIP Conf. Proc.* **2022**, *2445*, 30020.
[43] T. Hirsch, A. Khenissi, *Energy Procedia* **2014**, *49*, 1165.
[44] F. J. Sorbet, M. H. de Mendoza, J. García-Barberena, *AIP Conf. Proc.* **2019**, *2126*, 30056.
[45] *SpiCoPV Project. Zuwendungsgeber: Bundesministerium für Wirtwschaft und Klimaschutz aufgrund eines Beschlusses des Deutschen Bundestages, Förderkennzeichen: 03EE5087A.*
[46] A. Asgharzadeh, B. Marion, C. Deline, C. Hansen, J. S. Stein, F. Toor, *IEEE J. Photovolt.* **2018**, *8*, 798.
[47] Verband Deutscher Maschinen- und Anlagenbau (VDMA), *International Technology Roadmap for Photovoltaic* **2021**.
[48] R. Shigenobu, M. Ito, H. Taoka, *Energy Rep.* **2021**, *7*, 7004.